J. Membrane Biol. 19, 277–303 (1974)
© by Springer-Verlag New York Inc. 1974

Statistical Analysis of Alamethicin Channels in Black Lipid Membranes

Günther Boheim

Fachbereich Biologie, Universität Konstanz, 775 Konstanz, Germany

Received 24 April 1974; revised 26 June 1974

Summary. Pore formation of alamethicin has been studied by the analysis of steady-state fluctuations of single-pore conductances. An aggregation model is proposed where transitions to the next higher or lower pore state occur by uptake or release of one monomer. It is assumed that alamethicin forms an elongated loop in the bilayer. The main voltage-dependent step is the insertion of this monomer into the membrane after complexation with a cation. This mechanism is equivalent to dipole orientation in an electric field. Pore formation is restricted by the energy required to enlarge the channel in the membrane.

Since Mueller and Rudin (1968) reported on action potentials and oscillations induced by alamethicin in black lipid membranes, considerable progress has been made in examining the properties of this macrocyclic polypeptide antibiotic. The observation of discrete conductance steps has given evidence that certain substances are able to create ion-permeable pores in lipid bilayers. These pores open and close in a statistically random manner. Bean, Shepherd, Chan and Eichner (1969) and Ehrenstein, Lecar and Nossal (1970) described the pore formation properties of excitability inducing material (EIM). Hladky and Haydon (1970) demonstrated conductance fluctuations induced by gramicidin A in black lipid films. Alamethicin has been shown by Gordon and Haydon (1972) and in an extensive report by Eisenberg, Hall and Mead (1973) to be a pore former, too. In contrast to EIM and gramicidin A, which mainly show fluctuations between two conductance states, the alamethicin pore exhibits up to five conductance levels in bacterial phosphatidylethanolamine-*n*-decane membranes (Eisenberg *et al.*, 1973) and up to seven levels in glyceryl monooleate-*n*-decane membranes (Gordon & Haydon, 1972).

While the primary structure of EIM is not yet known, a series of π_{LD}-helices for gramicidin A dimer pores has been proposed by Urry (1971) and

Urry, Goodall, Glickson and Mayers (1971). Concentration-dependent relaxation experiments by Bamberg and Läuger (1973) gave strong evidence for this dimer concept. For alamethicin, no detailed model of pore structure has been proposed and the situation seems to be quite complicated.

Theory

Statistics of Current Fluctuations

The general appearance of current fluctuations generated by transitions of a single channel between its different conductance states is represented schematically in Fig. 1. From the current record $J(t)$ a number of parameters may be obtained which are used in the further analysis of the system. The single channel conductance Λ_ν in state ν is defined as the ratio of current J_ν through the channel in the ν^{th} conductance state (total current minus bare membrane current, *see* Fig. 1) divided by voltage V:

$$\Lambda_\nu = \frac{J_\nu}{V}. \tag{1}$$

If t_{obs} is the observation time (which is assumed to be large) and t_ν the total time spent by the channel in state ν during t_{obs}, the probability

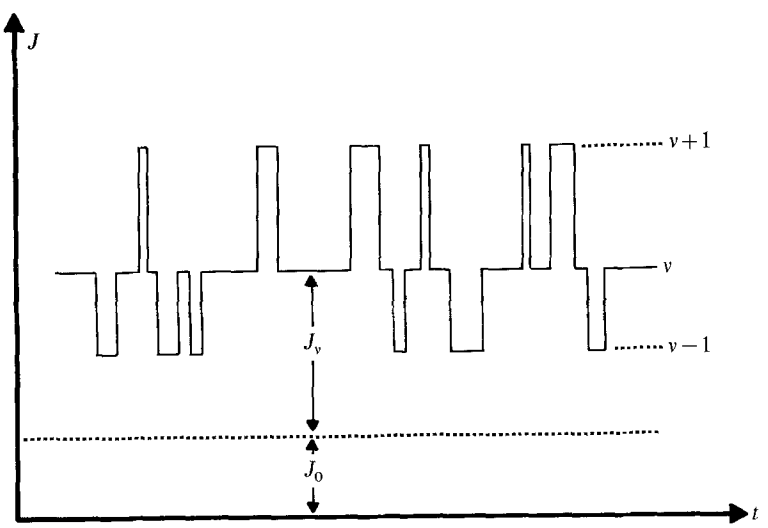

Fig. 1. Fluctuation of membrane current J as a function of time t in the presence of a single conducting channel. For simplicity, only three conducting states $(\nu-1)$, ν, $(\nu+1)$ of the channel are shown. J_0 is the current through the bare membrane. Schematic

p_v of state v is given by

$$p_v = \frac{t_v}{t_{obs}}. \tag{2}$$

If state v occurs z_v times during t_{obs} the mean lifetime τ_v of state v is defined by

$$\tau_v = \frac{t_v}{z_v}. \tag{3}$$

Finally, we introduce the mean number $\sigma_{v,v+1}$ of transitions from state v to state $v+1$ occurring in one second; correspondingly, $\sigma_{v+1,v}$ is the number of transitions from state $v+1$ to state v. Under steady-state conditions the relation

$$\sigma_{v,v+1} = \sigma_{v+1,v} \tag{4}$$

holds. We assume that transitions $v \to (v \pm 2)$, etc. do not occur. Since, then, state v is created either by a transition $(v+1) \to v$ or by a transition $(v-1) \to v$ and is terminated either by $v \to (v+1)$ or by $v \to (v-1)$, it is easy to see that

$$\frac{z_v}{t_{obs}} = \frac{1}{2}(\sigma_{v,v-1} + \sigma_{v,v+1} + \sigma_{v-1,v} + \sigma_{v+1,v}). \tag{5}$$

Together with Eqs. (2)–(4) we obtain

$$p_v = \tau_v(\sigma_{v,v-1} + \sigma_{v,v+1}). \tag{6}$$

This relation must always be fulfilled independent of any particular model. It may therefore be used as a check of consistency of the analysis.

Formal Analysis of the Channel Model

The model which we will use for the interpretation of the experimental results is based on the following assumptions. If a lipid membrane is in contact with an aqueous alamethicin solution, alamethicin molecules become adsorbed at the membrane-solution interface. In the adsorbed state the alamethicin molecule may form a complex with a cation from the aqueous solution, whereby part of the primary hydration shell of the ion is replaced by amide carbonyls of the peptide. A likely conformation of the alamethicin molecule at the interphase between hydrophilic and hydrophobic regions is that of an elongated flat loop stabilized by intramolecular hydrogen bonds (Fig. 2). If a voltage is applied to the membrane (alamethicin solu-

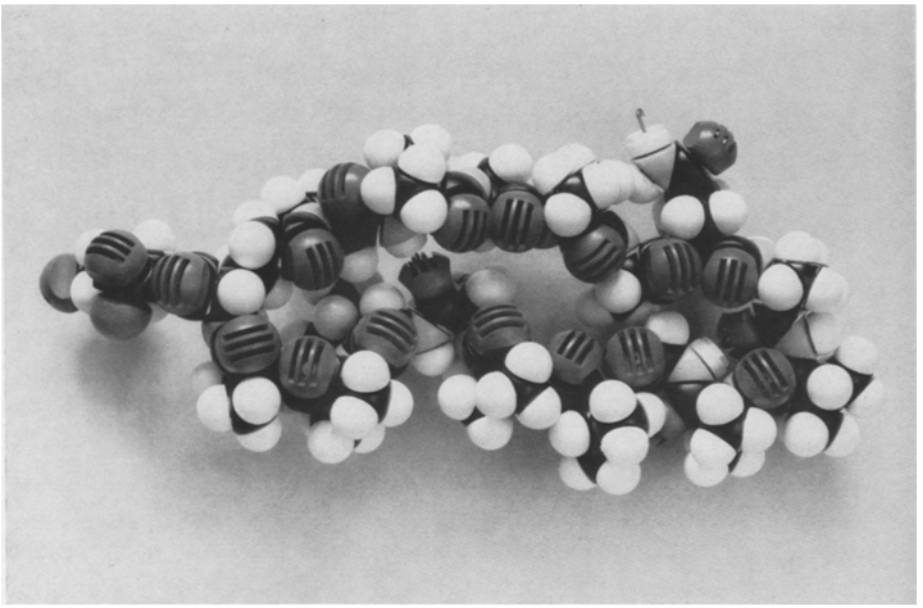

a

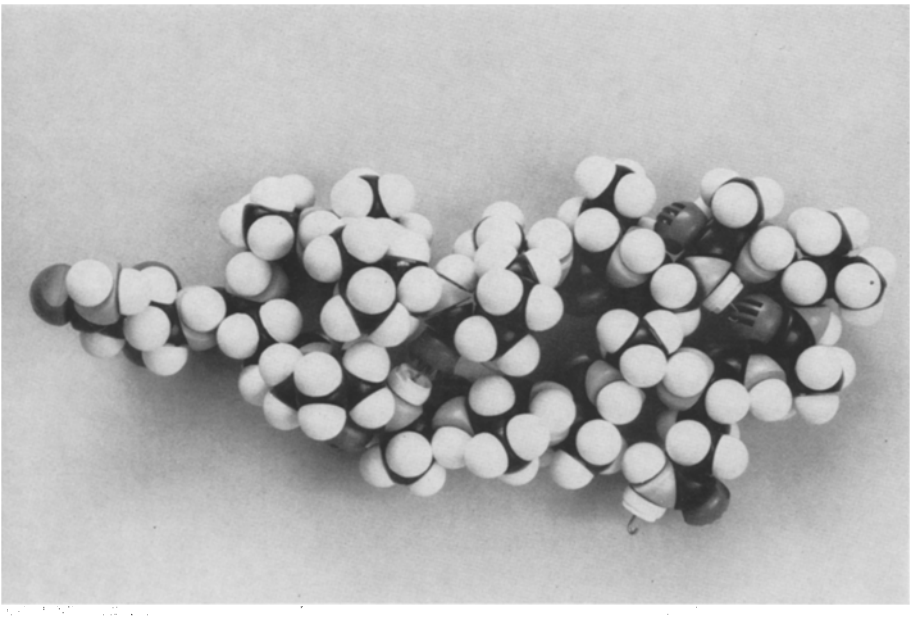

b

Fig. 2. A likely conformation of the alamethicin molecule at the interface between hydrophobic and hydrophilic regions. The CPK model shows an elongated flat loop stabilized by intramolecular hydrogen bonds. One side of the molecule (*a*) exhibits two strings of carbonyl oxygens, whereas on the other side (*b*) the hydrophobic residues of the amino acids are pointing outwards. Loop configurations different from the proposed one are not excluded and may be possible

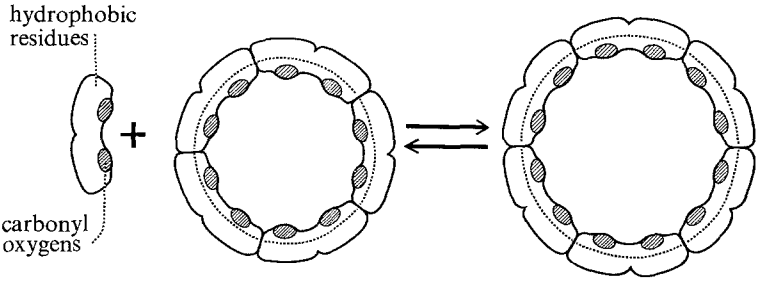

Fig. 3. Aggregation pore model of alamethicin which shows transitions between channels of different size by uptake or release of one monomer. The channel is shown end-on (perpendicular to the membrane surface). Schematic

tion positive), an electrical driving force is generated, which tends to turn the positively charged end of the molecule into the hydrophobic interior of the membrane. It is assumed that the molecule in this state possesses a tendency to aggregate laterally, forming dimers, trimers, tetramers and so forth (Fig. 3). From molecular models it is seen that polar and apolar groups of alamethicin may be arranged in such a way that the interior of the aggregate becomes hydrophilic whereas the hydrophobic residues of the aminoacids are pointing outwards. A basically similar structure has been proposed by Finkelstein and Holz (1973) for pores created by polyene antibiotics. In this way, higher aggregates form hydrophilic channels extending through the membrane. The length of the channel would be about 30 to 34 Å, which is near the lower limit of membrane hydrophobic thickness. A similar situation occurs with gramicidin A, where the channel presumably is formed by head-to-head association of two π^6_{LD}-helices (Urry, 1972), giving a length of 25 to 30 Å. In the above model the different conductance states of the alamethicin channel are represented by a sequence of aggregates with different numbers of monomers and therefore different pore diameters. Transitions between neighboring conduction states then arise from uptake or release of one monomer by the aggregate. The lowest observable conductance state may be the trimer or the tetramer, but for the moment this assignment is not critical.

The rates of association and dissociation of aggregates are described by rate constants $k_{\nu,\nu+1}$ and $k_{\nu,\nu-1}$, respectively. If N_ν is the concentration of the aggregate corresponding to the ν^{th} conductance state and N the monomer concentration in the membrane (both expressed in mol cm^{-2}), then the rate of change of N_ν is given by

$$\frac{dN_\nu}{dt} = k_{\nu-1,\nu} N_{\nu-1} N - k_{\nu,\nu-1} N_\nu - k_{\nu,\nu+1} N_\nu N + k_{\nu+1,\nu} N_{\nu+1}. \tag{7}$$

In the equilibrium state of the system $\left(\frac{dN_v}{dt}=0\right)$ each partial reaction is in equilibrium according to the principle of microscopic reversibility so that

$$\frac{N_v}{N_{v-1}N}=\frac{k_{v-1,v}}{k_{v,v-1}}=K_v. \tag{8}$$

(It should be emphasized that for any given voltage a true equilibrium state with respect to the concentrations N_v is reached at sufficiently long times, even if an electrical current flows through the channels.) The equilibrium constant K_v may be expressed by the probabilities p_v [Eq. (2)], if we use the fundamental statistical assumption that time average is equal to ensemble average:

$$p_v=\frac{t_v}{t_{\text{obs}}}=\frac{N_v}{N_p}. \tag{9}$$

($N_p=\sum_{v=0}^{\infty}N_v$ is the total concentration of conducting and nonconducting channels per cm^2.) Eq. (8) may then be written in the form

$$K_vN=\frac{p_v}{p_{v-1}}. \tag{10}$$

K_vN may therefore be obtained directly from the experimental current record. From the definition of $k_{v,v-1}$ [Eq. (7)] it is seen that $k_{v,v-1}N_v$ is the number of transitions $v\to(v-1)$ per cm^2 of membrane per second. Accordingly, $k_{v,v-1}N_v/N_p$ is the number of transitions per channel per second:

$$\sigma_{v,v-1}=\frac{k_{v,v-1}N_v}{N_p}. \tag{11}$$

Together with Eq. (9) one finds:

$$k_{v,v-1}=\frac{\sigma_{v,v-1}}{p_v}. \tag{12}$$

This equation may be used for the calculation of rate constants for transitions to the next lower state from experimental data.

In many cases the determination of mean lifetimes τ_v is difficult, because events of short duration tend to be suppressed in the current records due to limited time resolution of the measuring system. For this reason an alternative procedure has been used for the evaluation of τ_v. This method is

based on the assumption that transitions from state v to states $v+1$ or $v-1$ occur at random; i.e., independent of the previous history of the channel.

If we assume all channels of an ensemble to exist in state v (i.e. $N_v \neq 0$, $N_{k \neq v} = 0$) at $t = 0$ and consider the transition processes without back reaction, we obtain from Eq. (7):

$$\frac{dN_v}{dt} = -k_{v,v-1} N_v - k_{v,v+1} N \cdot N_v. \tag{13}$$

Under the assumption that N is large enough not to change during the analysis, a simple exponential dependence results

$$N_v(t) = N_v(0) \exp\left(-\frac{t}{\tau_v}\right) \tag{14}$$

with

$$\tau_v = \frac{1}{k_{v,v-1} + k_{v,v+1} \cdot N}.$$

The statistical assumption involves that $N_v(t)$ is equivalent to the number of events $n_v(t)$ (occurrences of state v) with a lifetime longer than t in the fluctuation pattern of a single channel. Thus, τ_v may be obtained by plotting $\ln [n_v(t)]$ as a function of t.

In the following we present some new results on steady-state conductance fluctuations in the presence of alamethicin. These measurements have been performed at reduced temperatures, so that the duration of the fluctuations became sufficiently long to allow a detailed statistical analysis. The measurements are analyzed in terms of a model which represents the pore as an oligomer of alamethicin. The diameter of the pore depends on the number of alamethicin molecules in the pore. The transitions between the different conductance states correspond to the uptake or release of one alamethicin molecule from the oligomer. This model has been discussed for some time by M. Delbrück, J. E. Hall, M. Eisenberg and G. Christoph and also by P. Mueller and G. Baumann (*personal communications*).

Materials and Methods

Black lipid membranes were formed from bovine brain phosphatidylserine (Koch-Light Ltd.) repurified by column chromatography and from dierucoyl-L-α-phosphatidylcholine (di-(22:1)-lecithin) synthesized by K. Janko (Benz, Stark, Janko & Läuger, 1973). Membrane-forming solutions were made of 0.3% (w/v) phosphatidylserine and 1% (w/v) di-(22:1)-lecithin in *n*-decane, respectively.

Alamethicin was purchased from Microbiological Research Establishment, Porton Down, Salisbury. The original alamethicin provided by Dr. G. B. Whitfield, Upjohn Co., Kalomazoo, Michigan has been shown by Melling and McMullen (1974) to be a mixture of three components. By thin-layer chromatography with chloroform/methanol/water (65:24:4 v/v/v) they found a main component with an Rf value of 30 comprising about 85% of the natural alamethicin, a second component (~12%) at Rf 50 and a third (~2%) at Rf 20. The primary structure published by Payne, Jakes and Hartley (1970) seems to be that of the main component. The primary structure of the Rf 50 and Rf 20 components is not yet known.

We have made our experiments with the pure Rf 30 fraction of alamethicin and with the pure Rf 50 fraction. Alamethicin was added from ethanolic stock solutions of 10^{-4} or 10^{-5} g/ml, respectively, in amounts of 10 to 20 μliters to about 7 ml aqueous solution on one side of the membrane only.

Protamine (salmine sulfate, pure grade) was purchased from Serva, Heidelberg. The sample, a natural mixture of several salmine components, has been checked for purity by SDS gel electrophoresis and amino acid analysis with the help of L.E. Hood at the California Institute of Technology.

Salt solutions were 1 M KCl. In the case of phosphatidylserine membranes the salt solutions were buffered at pH 7 with 5 mM Tris at 3 °C. With di-(22:1)-lecithin membranes, unbuffered salt solutions at pH ~6 were used at 11 °C.

The measuring cells were made from Teflon with a glass window to observe the membrane. The wall separating the two aqueous compartments contained a hole of 0.4 mm diameter allowing formation of membranes with an area of about 0.1 mm^2. The cell was adapted to a thermostated metal block. Both were inserted into an aluminum box for electrical shielding. This box was mounted onto a stone slab, which in turn rested on a motorcycle innertube for mechanical isolation, The aqueous solutions were stirred by Teflon-coated steel bars. Because of electrical noise, stirring was stopped during the current measurements and time allowed for the system to reach equilibrium.

The electrical measuring system was built into a shielded box in solid connection with the cell box and mounted on the same stone slab. The electrical circuit included a voltage source supplied by a battery, a differential voltmeter and a current amplifier (voltage clamp design) with a feedback resistor of $5 \times 10^7 \Omega$. The amplifiers used were Type 42K or 42L from Analog Devices, Norwood, Mass. The electronic design followed to some extent the design of Eisenberg (1972). Because of the small membrane area, the background noise amplitude could be reduced to 2×10^{-13} amps at a response time of 10 msec and to 2×10^{-12} amps at a response time of 1 msec. Current and voltage were measured separately with four Ag/AgCl electrodes.

Voltage will be designated positive if the more positive potential is applied on the side of alamethicin addition. Current direction is defined as positive for cation transfer from the alamethicin-containing compartment to the opposite one.

The current fluctuations were recorded on a tape recorder (Precision Instruments, Palo Alto, Calif., Type PI-6200). From the tape, paper records were made on a UV-recorder (Honeywell Visicorder Type 2208 A) or in case of slow fluctuations on a strip chart recorder (Hewlett Packard Type 7100 BM). Tape speed could be reduced by a factor of 10 or 100 during the transfer to the paper recorder. This record allowed an accurate evaluation of the fluctuation pattern over at least two decades of time.

Results

To establish that no more than a single pore is present and that the pore fluctuates in a stationary state, the following criteria have been used:

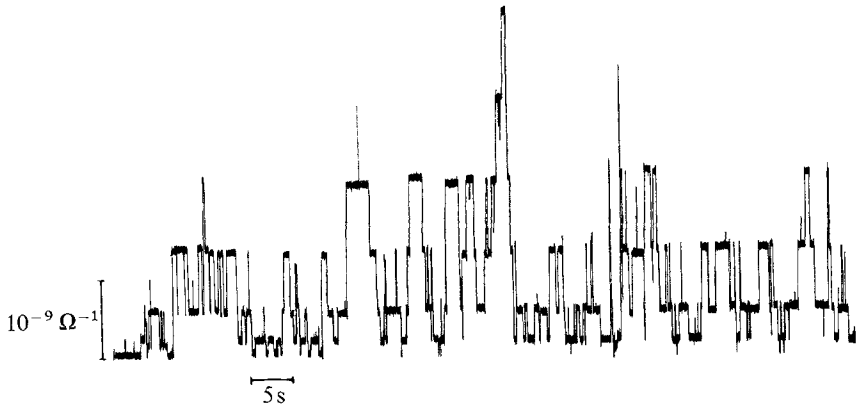

Fig. 4. Current fluctuations of an alamethicin-doped black lipid membrane as a function of time in the presence of a single conducting channel. Note gradual start of fluctuations at constant applied voltage. After a few seconds a stationary fluctuation state is attained. Up to six levels above bare membrane conductance can be observed. Membrane solution: 0.3% phosphatidylserine in *n*-decane. Salt solution: 1 M KCl; pH 7, 5 mM Tris buffer. Antibiotic concentration: 3×10^{-8} g/ml alamethicin Rf 30 to one compartment only. Temperature: 3 °C. Applied voltage: 90 mV

(a) A single pore is active if a specific pattern of conductance levels is observed. A continuous record showing this particular sequence of conductance steps which are never multiples of a unit step, is represented in Fig. 4. Differences between neighboring conductance states increase toward higher conductances and seem to approach an upper limit. Deviations from this pattern indicate the presence of additional pores.

(b) For a check that the pore is in a stationary state the following procedure has been used. The total observation time is divided into intervals of duration Δt. Within each interval a mean conductance state ν is calculated from the current record according to

$$\bar{\nu}=\frac{1}{\Delta t}\sum_i \nu_i t_i. \tag{15}$$

ν_i is the state number of event i, beginning with $\bar{\nu}=0$ for the conductance of the bare membrane, $\nu=1$ for the first conductance state, and so forth. t_i is the duration of event i. The summation is carried out over all events during Δt. Δt is chosen to be about 20 times the mean lifetime of the most probable conductance state. If the pore is in a steady state, a plot of $\bar{\nu}$ versus time t should show random fluctuations without systematical trend. An example is given in Fig. 5.

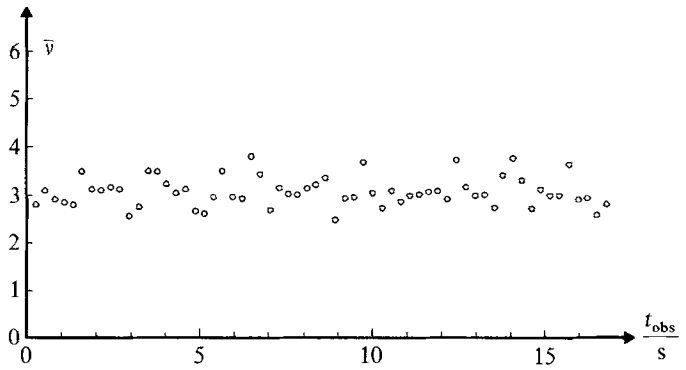

Fig. 5. Statistical variation with time of small interval mean number of conductance levels $\bar{\nu}$ in equilibrium. The time interval was chosen to be $\Delta t = 270$ msec. For explanation of $\bar{\nu}$ and t_{obs} *see text*. Membrane solution: 1 % di-(22:1)-lecithin in *n*-decane. Salt solution: 1 M KCl, unbuffered. Antibiotic concentration: 1.5×10^{-7} g/ml alamethicin Rf 30 to one compartment. Temperature: 11 °C. Applied voltage: 63 mV

From steady-state fluctuations of the type shown in Fig. 4, four different statistical parameters may be extracted which are not all independent [compare Eq. (6)]:

(1) the conductance value Λ_ν of each pore state;

(2) the probability p_ν of conductance state ν as given by the ratio of total time which has been spent by the pore in state ν during observation time t_{obs}, divided by t_{obs} [Eq. (2)];

(3) the number of transitions per unit time from state ν to state $\nu - 1$ ($\sigma_{\nu,\nu-1}$) and from state ν to state $\nu + 1$ ($\sigma_{\nu,\nu+1}$);

(4) the lifetimes of individual events in a given conductance state.

Steps which extend over two or three states have been counted as steps via unresolvable intermediate states. We found two kinds of kinetic behavior of the conductance state of the bare membrane. During steady-state fluctuations of a pore the conductance occasionally drops down to the conductance of the bare membrane and after a short time again jumps into higher levels. This behavior is in sharp contrast to the periods of ground-level conductance between the occurrences of individual pores. The observation of the ground-state conductance during pore fluctuations indicates that a pore state of zero conductance exists.

The results of the statistical analysis are listed in Tables 1–6. For the specification of the experimental conditions the following notation has been used in the Tables:

PC: di-(22:1)-lecithin membrane in 1 M KCl at 11 °C. To one aqueous compartment 1.5×10^{-7} g/ml alamethicin (Rf 30 fraction) was added. Three different voltages (28, 63, 100 mV) were applied to the same membrane.

PS/30, PS/50: phosphatidylserine membrane in 1 M KCl, pH 7, at 3 °C. To one compartment 3×10^{-8} g/ml alamethicin of the Rf 30 fraction (PS/30) or of the Rf 50 fraction (PS/50) were added.

PS/pr: phosphatidylserine membrane in 1 M KCl, pH 7, at 3 °C. After the addition of 3×10^{-8} g/ml alamethicin of the Rf 30 fraction to one aqueous compartment, 10^{-7} g/ml protamine was added to both sides. The same membrane was used for the measurement at both voltages (60 and 80 mV).

In all cases the positive voltage was applied to the alamethicin side. In the case of the di-(22:1)-lecithin membrane the pore was formed at 120 mV, the characteristic voltage defined by Eisenberg *et al.* (1973), and then the voltage reduced to 63 mV. After the current fluctuations were recorded at this voltage, the voltage was changed to 28 mV and thereafter to 100 mV. In each case the record of the current fluctuation was started a few seconds after the voltage change in order to allow the pore to come into a stationary state.

With phosphatidylserine membranes in the presence of protamine the pore-forming procedure was the same. First fluctuations at 60 mV, then at 80 mV were recorded. In the experiments with phosphatidylserine membranes without protamine, pore formation was induced at 90 mV, and the current fluctuations measured at the same voltage.

The difference between these two pore-forming procedures is the following: The relatively fast voltage increase up to the "characteristic voltage" usually induces several pores. While reducing the membrane voltage sometimes all pores close except one, which may stay fluctuating over a few minutes. This may be due to a high activation barrier for the pore decay and the small thermal energy at the low temperature. On the other hand, pore formation at a given voltage reflects the strong voltage dependence of the rates of pore formation and decay. We observed pores of different duration, periods with no pore or two pores according to a statistical distribution. For our evaluations we chose a long trace of single pore fluctuations in each case.

Whereas the first procedure is suitable to investigate the voltage dependence of pore state distributions, the second one gives the possibility of a complete analysis of alamethicin pore formation.

Table 1. Single-channel conductances Λ_v of state v [Eq. (1)] in $10^{-10}\,\Omega^{-1}$. (For further explanations *see text.*)

State	PC 28 mV	PC 63 mV	PC 100 mV	PS/30 90 mV	PS/50 60 mV	PS/pr 60 mV	PS/pr 80 mV
1	0.43	0.45		1.2	0.65	1.0	
2	2.4	2.4	2.4	5.2	4.0	4.8	4.8
3	5.9	6.1	6.5	13.2	11.3	12.7	12.9
4	10.5	10.8	11.3	22.2	19.3	21.8	22.0
5	15.4	16.0	16.5	31.8	27.9	31.6	31.7
6		21.5	21.9	42.0	37.0	41.8	42.1
7							52.6
Λ_2/Λ_1	5.6	5.3		4.3	6.2	4.8	
Λ_3/Λ_2	2.46	2.54	2.71	2.54	2.83	2.65	2.69
Λ_4/Λ_3	1.78	1.77	1.74	1.68	1.71	1.72	1.71
Λ_5/Λ_4	1.47	1.48	1.46	1.43	1.45	1.45	1.44
Λ_6/Λ_5		1.34	1.33	1.32	1.33	1.32	1.33
Λ_7/Λ_6							1.25

Table 1 shows the single-channel conductance values Λ_v of the different states, as well as the ratios Λ_{v+1}/Λ_v. As discussed later, these ratios may be explained by the proposed pore model. In the case of Montal-Mueller membranes with di-(22:1)-lecithin, but otherwise identical conditions as the PC set, the values of Λ_{v+1}/Λ_v are about the same, although the absolute conductance values are increased by a factor of 2.5 (G. Boheim, *unpublished results*).

Table 2 shows distributions of pore level probabilities p_v, which are obtained from the current record according to Eq. (2).

In addition to the p_v, Table 2 also contains the values of $K_v N = p_v/p_{v-1}$ and the ratios K_v/K_{v+1} of the equilibrium constants which are given by [compare Eq. (10)]:

$$\frac{K_v}{K_{v+1}} = \frac{(p_v)^2}{p_{v-1}\,p_{v+1}}. \tag{16}$$

It is seen that for each type of membrane the ratio K_v/K_{v+1} is almost voltage independent, and is also largely independent of v.

Fig. 6 shows a semi-log plot of the product $K_v N$ for the PC membranes versus voltage. If we write the slope m_v of log (NK_v) as

$$m_v = \alpha_v \frac{F}{RT} \tag{17}$$

(F = Faraday constant, R = gas constant, T = absolute temperature), a mean value of $\bar{\alpha} = 0.93$ is obtained. Stronger deviations from the mean in

Table 2. Probabilities p_ν of conductance state ν [Eq. (2)], expressed in per cent. In addition, the values of NK_ν and $K_\nu/K_{\nu+1}$, as calculated from Eq. (12), are given

State	PC 28 mV	PC 63 mV	PC 100 mV	PS/30 90 mV	PS/50 90 mV	PS/pr 60 mV	PS/pr 80 mV
0	0.47	0.035		9.1	1.3		
1	15.9	1.79	0.06	21.6	12.4	1.3	0.3
2	50.0	21.5	3.13	32.0	21.9	12.8	5.9
3	30.0	49.6	29.1	21.1	32.8	41.2	26.8
4	3.54	23.7	49.0	12.3	24.5	34.7	42.6
5	0.09	2.44	17.9	3.4	6.4	9.4	20.8
6		0.053	0.89	0.5	0.7	0.6	3.3
7							0.3
NK_1	33.9	51.1		2.37	9.5		
NK_2	3.14	12.0	52.1	1.48	1.77	10.7	19.7
NK_3	0.60	2.31	9.3	0.659	1.50	3.22	4.55
NK_4	0.118	0.477	1.68	0.583	0.75	0.84	1.59
NK_5	0.025	0.103	0.366	0.276	0.26	0.273	0.488
NK_6		0.022	0.050	0.147	0.115	0.071	0.157
NK_7							0.084
K_1/K_2	10.8	4.3		1.60	5.4		
K_2/K_3	5.2	5.2	5.6	2.25	1.2	3.3	4.3
K_3/K_4	5.1	4.8	5.5	1.13	2.0	3.8	2.9
K_4/K_5	4.7	4.6	4.6	2.11	2 9	3.1	3.3
K_5/K_6		4.7	7.3	1.88	2.3	3.8	3.1
K_6/K_7							1.9

Table 3. Transition frequencies $\sigma_{\nu,\nu+1}=\sigma_{\nu+1,\nu}$ in $\sec^{-1}$. In addition, the total number $z=\sum_\nu z_\nu$ of recorded events is indicated

$\sigma_{\nu,\nu+1}$	PC 28 mV	PC 63 mV	PC 100 mV	PS/30 90 mV	PS/50 90 mV	PS/pr 60 mV	PS/pr 80 mV
σ_{01}	1.08	0.118		0.322	0.690		
σ_{12}	16.1	3.31	0.241	0.608	2.74	0.372	0.241
σ_{23}	18.0	16.0	4.89	0.470	3.47	2.76	6.45
σ_{34}	4.21	20.0	21.6	0.184	1.91	3.29	15.2
σ_{45}	0.241	5.32	24.6	0.0553	0.617	1.91	9.16
σ_{56}		0.472	4.72	0.0092	0.109	0.106	1.87
σ_{67}							0.241
z	1318	1530	1384	358	1050	318	1102

the case of $\nu=1$ and $\nu=6$ may be explained by the limited accuracy due to the observed events ($p_\nu<1\%$). A similar plot for PS membranes with protamine from Table 2 gives a mean value of $\bar{\alpha}=0.73$. The displacement of

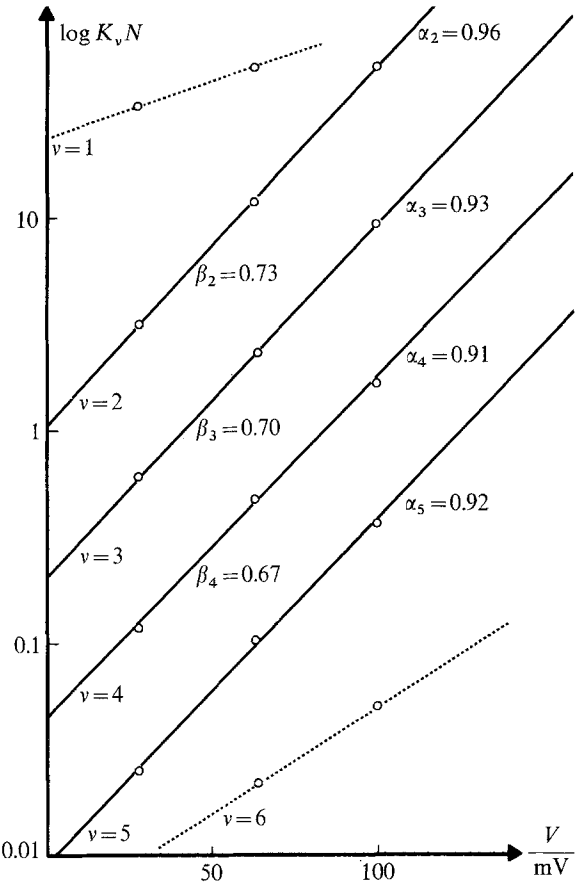

Fig. 6. Semi-log plot of distribution constants $K_\nu N$ versus voltage (PC sets of Table 2) showing voltage dependence of $K_\nu N$ and nearly voltage independence of $K_\nu/K_{\nu+1}$. Slope of solid straight lines is nearly the same in cases $\nu = 1, 2, 3, 4$. For explanation of α_ν and β_ν *see text*. Experimental conditions same as in Fig. 5

two neighboring straight lines with respect to the ordinate may be expressed by $\beta_\nu = \log(K_\nu/K_{\nu+1})$. A mean value $\bar{\beta} = 0.7$ is found in Fig. 6, which corresponds to $\overline{(K_\nu/K_{\nu+1})} = 5.0$.

Table 3 gives values for $\sigma_{\nu,\nu-1} = \sigma_{\nu-1,\nu}$, the mean number of transitions occurring in one second between states ν and $\nu - 1$. Mean lifetimes τ_ν evaluated from the plot log $[n_\nu(t)]$ versus t according to Eq. (14) are listed in Table 4. As an example, log $[n_\nu(t)]$ is shown for a PC membrane at three different voltages in Fig. 7. In all cases an exponential behavior is found. The result of the consistency check is shown in Table 5. According to Eq. (6), probabilities p_ν have been calculated with values for $\sigma_{\nu,\nu-1}$ and τ_ν from

Table4. Mean lifetimes τ_v in msec, as evaluated from the log$[n_v(t)]$ versus t plot [Eq. (14)]. Examples of log $[n_v(t)]$ are given in Fig. 7

State	PC 28 mV	PC 63 mV	PC 100 mV	PS/30 90 mV	PS/50 90 mV	PS/pr 60 mV	PS/pr 80 mV
0	3.2			202	19.8		
1	8.0	4.8		259	30.5	32.8	
2	13.7	9.5	5.2	341	36.1	42.3	7.7
3	12.7	12.4	9.7	405	66.4	67.7	12.5
4	7.6	9.0	9.5	556	110.4	57.3	18.1
5		4.6	5.2	575	124.2	37.3	18.6
6			2.2				13.4

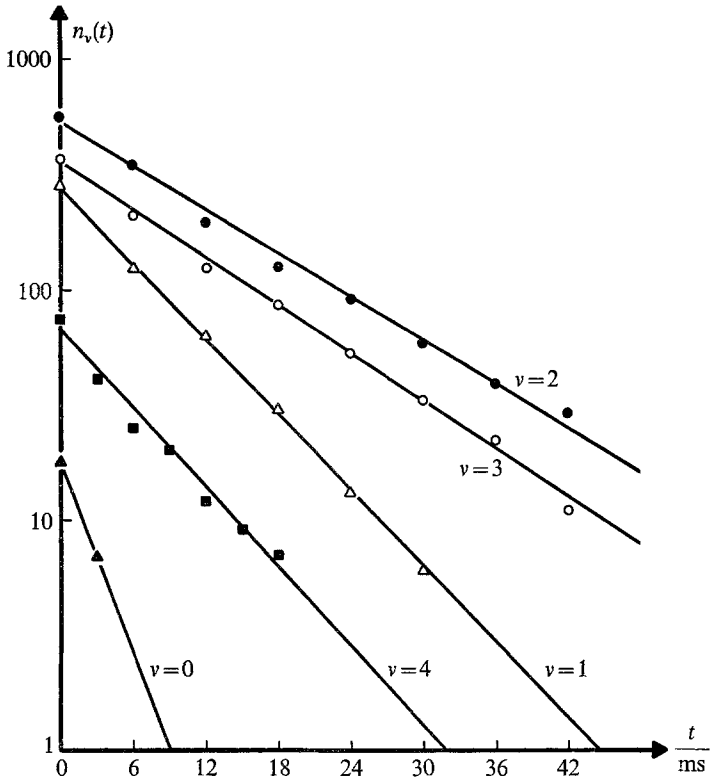

Fig. 7a

Fig. 7. Semi-log plot of $n_v(t)$ versus t (PC sets of Table 2) for determination of mean lifetime τ_v: (*a*) 28 mV; (*b*) 63 mV; (*c*) 100 mV. τ_v values are listed in Table 4. Experimental conditions same as in Fig. 5

Tables 3 and 4, respectively. Within the experimental error of about 10%, the p_v values of Tables 2 and 5 agree.

Table 6 contains the values of the rate constants $k_{v,v-1}$ for transitions to the next lower state which have been calculated from Eq. (12). Values for

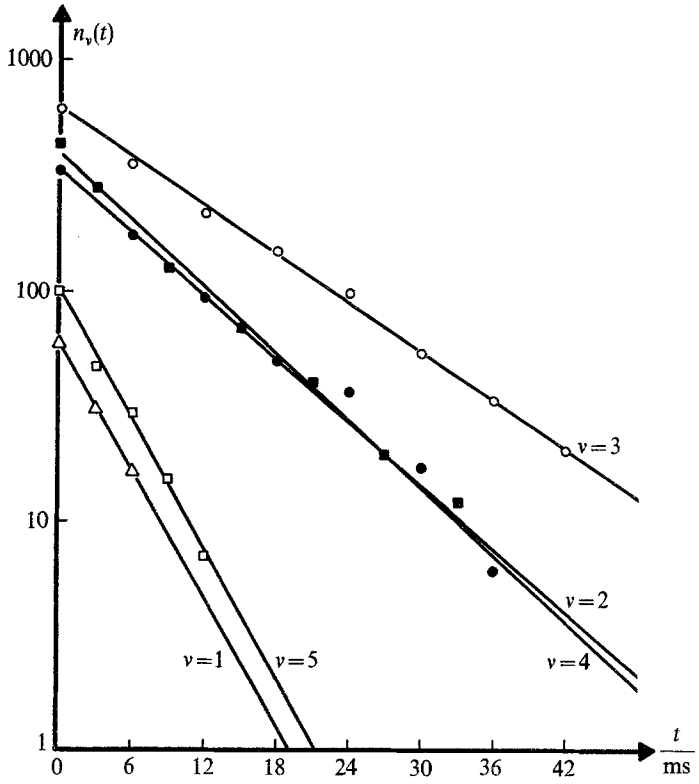
$n_v(t)$
1000
100
10
1
0
6
12
18
24
30
36
42
t
ms
$v=3$
$v=2$
$v=4$
$v=1$
$v=5$

Fig. 7b

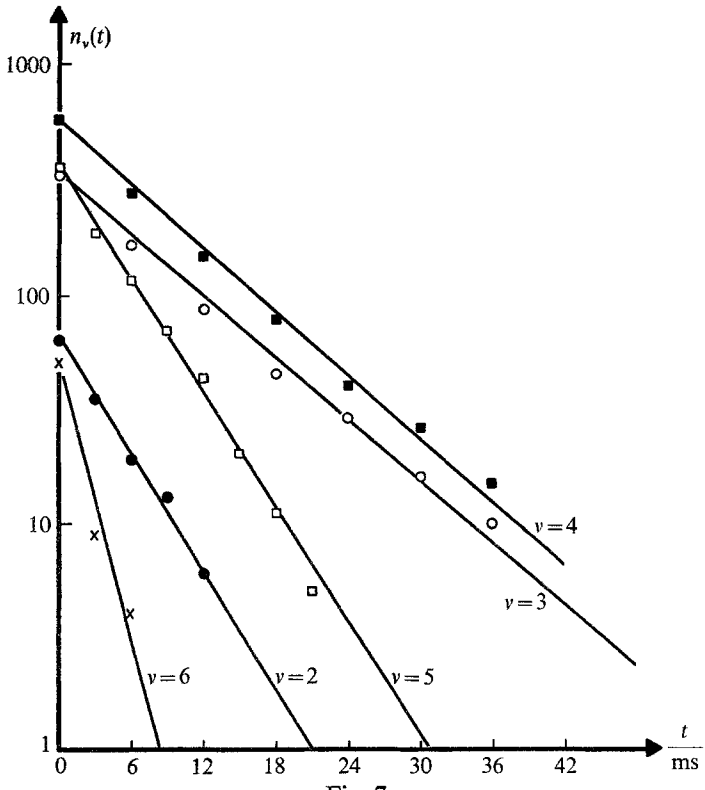
$n_v(t)$
1000
100
10
1
0
6
12
18
24
30
36
42
t
ms
$v=4$
$v=3$
$v=6$
$v=2$
$v=5$

Fig. 7c

Table 5. Consistency check of the analysis. The values of p_ν (in %) according to Eq. (6) from τ_ν and $\sigma_{\nu,\nu-1}$ are listed

State	PC 28 mV	PC 63 mV	PC 100 mV	PS/30 90 mV	PS/50 90 mV	PS/pr 60 mV	PS/pr 80 mV
0	0.35			6.51	1.37		
1	13.8	1.65		24.1	10.5	1.22	
2	46.7	18.3	2.67	36.8	22.4	13.2	5.15
3	28.2	44.6	25.7	26.5	35.7	41.0	27.1
4	3.38	22.8	43.9	13.3	27.8	29.8	44.2
5		2.66	15.0	3.68	9.02	7.53	20.5
6			0.92				2.83

Table 6. Rate constants $k_{\nu,\nu-1}$ of transitions to the next lower state, as calculated from Eq. (12). The $k_{\nu,\nu-1}$ are expressed in sec^{-1}.

$k_{\nu,\nu-1}$	PC 28 mV	PC 63 mV	PC 100 mV	PS/30 90 mV	PS/50 90 mV	PS/pr 60 mV	PS/pr 80 mV
k_{10}	6.8	6.6		1.5	5.6		
k_{21}	32.2	15.4	7.7	1.9	12.5	2.9	4.1
k_{32}	60.0	32.3	16.8	2.2	10.6	6.7	24.1
k_{43}	119	84.4	44.1	1.5	7.8	9.5	35.8
k_{54}	268	218	137	1.6	9.6	20.3	44.0
k_{65}		890	469	1.8	15.6	17.6	56.7
k_{76}							80.3

p_ν and $\sigma_{\nu,\nu-1}$ were taken from Tables 2 and 3, respectively. Whereas the rate constants in the case of di-(22:1)-lecithin membranes and of phosphatidylserine membranes with added protamine vary monotonously with ν, the $k_{\nu,\nu-1}$ values for phosphatidylserine membranes with alamethicin alone seem to show random deviations from a mean value.

The reproducibility of the experimental results is mainly limited by deviations of the alamethicin concentration in the aqueous solutions due to adsorption to the walls of the cell and also by changes in the lipid-to-decane ratio of the membrane (ageing effect). The ratios $K_\nu/K_{\nu+1}$ of the equilibrium constants generally show variations by 10 to 50% from membrane to membrane. Likewise, the absolute values of the mean lifetimes τ_ν may vary by a factor of $\leqq 2$. For this reason all parameters for a given set of experimental conditions have been measured with the same membrane.

Discussion

Within the framework of the proposed model it is assumed that the alamethicin molecule is adsorbed to the membrane interface as a monomer

and that it is in equilibrium with regard to cation complexation. Two methods of pore formation (same sort of a nucleation process) are feasible. Either the monomer with its positively charged end may be pulled into the membrane under the action of the voltage and then form oligomers by random association. Fluctuations in pore size occur by uptake or release of single monomers by the pores, these monomers in turn being in equilibrium with monomers at the interface. Alternatively, adjacent monomers at the interface may aggregate and then be pulled into the membrane. Additional monomers may be inserted directly into the oligomer pore by a "zipping" mechanism. This means that the monomer first enters the pore opening with its more positively charged part by enlarging it. Then like a zipper it opens this side of the channel while being inserted and closes it by itself. At the moment we cannot distinguish between these two possibilities.

An important problem is the molecular structure of the alamethicin in the pore. At least two possible structures may be envisaged. The first consists in an elongated loop, where two parallel strings of carbonyl-oxygens form one side of the molecule and the hydrophobic amino acid residues, form the opposite (Fig. 2). The negatively charged glutamin bound to the macrocyclic ring is situated on one end of the loop.

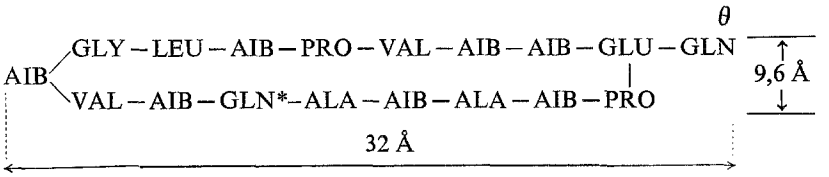

The cation may be complexed by carbonyl oxygens at an unspecified site of the molecule. But the probability of a monomer to be inserted into the membrane increases with the distance between the positive and negative charge, i.e. with the dipole moment of the molecule.

After insertion of the monomer into the membrane, the cation may be released on the other side. Thus, the alamethicin monomer may be introduced into a pore or return to the initial membrane side, where it is stabilized by the negatively charged amino acid. Alamethicin molecules whose negatively charged group has been methylated do not show this stabilization on the initial membrane interface, although pore formation occurs (J. E. Hall, *personal communication*; G. Baumann and P. Mueller, *personal communication*). The length of the loop channel in the above configuration has been estimated from the CPK molecule model to be ~ 32Å and the largest diameter normal to the extended loop ~ 9.6 Å.

Baumann and Mueller (*personal communication*) propose an alternative wedge-formed structure with only one string of carbonyl oxygens on one

side and a larger part with two turns of α-helical structure on the opposite. The complexed cation is situated away from the channel oxygens at the glutamin* residue and the negatively charged amino acid is located at one end of the wedge, too. The length of the channel would be ~26 Å and the largest diameter ~7.6 Å, respectively. Both structures of alamethicin are similar to a cylinder sector, well fitted to form cylindrical pores. Our estimates will be based on the loop model.

In the following we give an estimate for the inner diameter of the channel using a simple geometric approximation which may account for the peculiar sequence of the single channel conductance values in the different states of the pore.

We assume that the largest diameter a normal to the extended alamethicin loop is nearly constant for each pore state and determines the distance between the molecules forming the circular cross-section of a pore. The two strings of the alamethicin molecule are considered to be flexible to fit into a cylindrical shape. Therefore we may draw a circle with a circumference equal to the number of alamethicin molecules times a constant length a (Fig. 3). Then we may estimate the inner radii ρ_ν of the channel in the different states by assuming that the cross-sectional area A_c of each molecule within the drawn circle is constant. We estimate $A_c \approx 14$ Å^2 under assumption that the carbonyl oxygens in the dimer are nearly close-packed. Specifically, we use the same values for the oxygen-to-oxygen distances as Urry (1972) proposed for the π^4_{LD}-helix of gramicidin A, which gives an inner radius of $\rho_o \sim 0.7$ Å. This channel is too small to allow the passage of an alkali ion. Using $a = 9.6$ Å we determined the inner channel radii ρ_ν listed in Table 7 according to

$$\rho_\nu = \sqrt{\left(\frac{\nu+2}{2\pi}\right)^2 \cdot a^2 - \frac{\nu+2}{\pi} \cdot A_c}. \tag{18}$$

For the first conductive channel a diameter of 5.6 Å is obtained in this way which may be compared with the diameter of 4 Å of the conducting π^6_{LD}-helix of gramicidin A. This is consistent with the observation that the single-channel conductance of gramicidin A is lower under similar experimental conditions (Bamberg & Läuger, 1974).

In addition we have listed in Table 7 the ratios of two consecutive channel cross-sections. Under the assumption that the ion mobility in the pore is independent of the channel size, this ratio should be equal to the ratio of consecutive pore conductances. The reason for the discrepancy at lower oligomers might be an effect of the channel size on the ionic mobility in the channel. For other listed aggregates the calculated conductance ratios agree

Table 7. Estimated radii ρ_ν of inner channels of alamethicin pores. For comparison, channels volume ratios [equal to $(\rho_{\nu+1}/\rho_\nu)^2$] and pore conductance ratios $\Lambda_{\nu+1}/\Lambda_\nu$ of Table 1 (PC, 63 mV) have been listed

State	Molecules per pore	ρ_ν[Å]	$\left(\frac{\rho_{\nu+1}}{\rho_\nu}\right)^2$	$\frac{\Lambda_{\nu+1}}{\Lambda_\nu}$
0	2	0.7		
1	3	2.8	2.5	5.3
2	4	4.4	1.86	2.54
3	5	6.0	1.60	1.77
4	6	7.6	1.46	1.48
5	7	9.2	1.35	1.34
6	8	10.7	1.30	
7	9	12.2		

with the experimental values. For higher aggregates than the heptamer we observe a larger variation in pore state conductance distributions. This may cause lower ratios of the mean conductance values than expected, especially if these states are of very small probability. We think that sterical distortions from the cylindrical shape in the case of large channel diameters are responsible for the fact.

For the description of the different steps of pore formation we introduce a series of equilibrium constants K_m, K_o, K_1, ...:

$$N_s \underset{k_{ms}}{\overset{k_{sm}}{\rightleftarrows}} N; \quad K_m = \frac{k_{sm}}{k_{ms}} = \exp\left\{\frac{\alpha_m \cdot FV - \Delta G_m}{RT}\right\} \tag{19a}$$

$$N + N \underset{k_{om}}{\overset{k_{mo}}{\rightleftarrows}} N_o; \quad K_o = \frac{k_{mo}}{k_{om}} = \frac{1}{N^*} \exp\left\{\frac{\alpha_p \cdot FV - \Delta G_o}{RT}\right\} \tag{19b}$$

$$N_{\nu-1} + N \underset{k_{\nu,\nu-1}}{\overset{k_{\nu-1,\nu}}{\rightleftarrows}} N_\nu; \quad K_\nu = \frac{k_{\nu-1,\nu}}{k_{\nu,\nu-1}} = \frac{1}{N^*} \exp\left\{\frac{\alpha_p \cdot FV - \Delta G_\nu}{RT}\right\} \tag{19c}$$

$\nu = 1, 2, \ldots$.

with N_s: concentration of alamethicin monomers per cm² at the membrane interface

N_s : concentration of alamethicin monomers per cm² in the membrane

N_o : concentration per cm² of nonconducting dimers

N_ν : concentration per cm² of conducting oligomers in state ν

N^* : standard concentration in mol cm^{-2}

N_A : Avogadro constant

F : Faraday constant

R : gas constant

T : absolute temperature

V : applied voltage

$\alpha_m \cdot FV$: energy (per mol) due to the transfer of one elementary charge across the fraction α_m of the membrane thickness (orientation of the dipole)

$\alpha_p \cdot FV$: voltage dependent part of the energy (per mol) associated with the uptake and release of a monomer by the pore

ΔG_m : change in Gibb's free energy per mol associated with transfer of monomers from the interface into the membrane interior

ΔG_o : change in Gibb's free energy per mol associated with dimerization within the membrane phase

ΔG_ν : change in Gibb's free energy per mol associated with uptake and release of a monomer by the oligomer.

With

$$N = N_s \cdot \exp\left\{\frac{\alpha_m \cdot FV - \Delta G_m}{RT}\right\} \tag{20}$$

the product NK_ν is given by

$$K_\nu N = \frac{N_s}{N^*} \cdot \exp\left\{\frac{(\alpha_m + \alpha_p) \cdot FV - (\Delta G_\nu + \Delta G_m)}{RT}\right\} \tag{21}$$

$\nu = 0, 1, 2, \ldots$.

Introducing

$$\alpha_m + \alpha_p = \alpha \tag{22}$$

$$\frac{N_s}{N^+} \cdot \exp\left\{\frac{-(\Delta G_o + \Delta G_m)}{RT}\right\} = \Gamma \tag{23}$$

and assuming that ΔG_ν varies linearly with ν:

$$\Delta G_\nu = \Delta G_o + \nu \cdot \Delta G_R \tag{24}$$

we obtain

$$K_\nu N = \Gamma \cdot \exp\left\{\frac{\alpha \cdot FV - \nu \cdot \Delta G_R}{RT}\right\} \tag{25}$$

$\nu = 0, 1, 2, \ldots$.

The plot of $\ln(K_\nu N)$ versus voltage in Fig. 6 yields $\bar{\alpha} = 0.93$ in the case of di-(22:1)-lecithin membranes. In the case of phosphatidylserine membranes with protamine $\bar{\alpha} = 0.73$ is obtained. The ratio of equilibrium constants gives

$$\beta_\nu = \ln \frac{K_\nu}{K_{\nu+1}} = \frac{\Delta G_R}{RT}. \tag{26}$$

From the finding that β_ν is nearly independent of ν, the assumed linear variation of ΔG_ν with ν [Eq. (24)] seems to be justified. The following numerical values are obtained:

$$\text{PC} \quad : \quad \Delta G_R = 0{,}91 \text{ kcal mol}^{-1}, \quad \bar{\beta}_\nu = 1.61$$

$$\text{PS/30}: \quad \Delta G_R = 0{,}32 \text{ kcal mol}^{-1}, \quad \bar{\beta}_\nu = 0.59$$

$$\text{PS/50}: \quad \Delta G_R = 0{,}45 \text{ kcal mol}^{-1}, \quad \bar{\beta}_\nu = 0.83$$

$$\text{PS/pr}: \quad \Delta G_R = 0{,}65 \text{ kcal mol}^{-1}, \quad \bar{\beta}_\nu = 1.19$$

An interpretation of the ΔG_R values seems to be quite complicated because of the complex nature of pore formation. If A_ν is the pore cross-section in state ν, then the proposed model predicts that $\Delta A = A_{\nu+1} + A_{\nu-1} - 2A_\nu$ is independent of ν and given by $\Delta A \cdot N_A = 88 \text{ m}^2 \text{mol}^{-1}$. If we now make the assumption that ΔG_R is proportional to ΔA, we obtain the following values for the energy $\Delta G_R / \Delta A$ per unit area: PC = 43 erg cm^{-2}, PS/30 = 16 erg cm^{-2}, PS/50 = 22 erg cm^{-2}, PS/pr = 31 erg cm^{-2}.

An important test for the proposed model would be the investigation of the linear dependence of $K_\nu N$ on the interfacial alamethicin concentration N_S. Under the assumption that a distribution equilibrium between membrane interface and bulk aqueous phase exists and that the ΔG values are independent of alamethicin concentration, $K_\nu N$ should be proportional to the bulk alamethicin concentration. In practice, however, these experiments are difficult due to the lack of reproducibility of very low alamethicin concentrations in water, and have not yet been done.

Eisenberg *et al.* (1973) found the formation of the pore to be the step principally responsible for the voltage dependence of the conductance in alamethicin-doped bilayer membranes, whereas the mean pore conductance increased only slightly with voltage. We confirmed this finding by plotting the mean pore conductance

$$\bar{A} = \sum_\nu p_\nu \cdot A_\nu \tag{27}$$

versus voltage (Fig. 8). To a good approximation a linear voltage dependence was obtained in contrast to the strong exponential dependence of the macro-

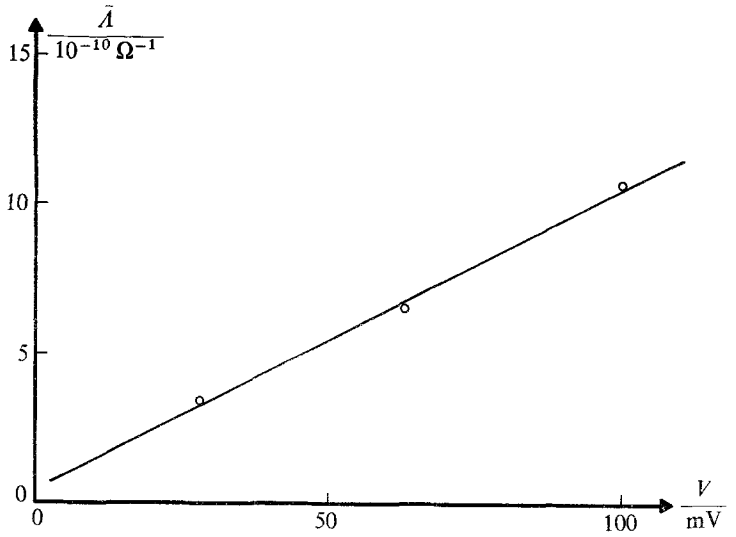

Fig. 8. Voltage dependence of the mean pore conductance $\bar{\Lambda}$ of a single pore. The mean pore conductance is defined by $\bar{\Lambda} = \sum_{\nu} p_\nu \cdot \Lambda_\nu$

scopic membrane conductance. This fact implies a high activation barrier for the pore formation step compared to the activation energies between the different pore states.

In the following we compare the expression for the oligomer concentration which is obtained from Eqs. (20)–(25):

$$N_\nu = N \cdot \Gamma^{\nu+1} \exp\left[(\nu+1)\frac{\alpha FV - \nu \Delta G_R/2}{RT}\right] \tag{28}$$

with the conductance formula of Eisenberg *et al.* (1973) for bacterial phosphatidylethanolamine membranes at 23 °C:

$$\lambda \sim (C_{al})^9 \cdot (C_{salt})^4 \cdot \exp\left\{6.5 \cdot \frac{FV}{RT}\right\} \tag{29}$$

and with the formula of Mueller and Rudin (1968) for sphingomyelin tocopherol membranes at 35 °C: [1]

$$\lambda \sim (C_{al})^6 \cdot (C_{salt})^{4.6} \cdot \exp\left\{5.5 \cdot \frac{FV}{RT}\right\}. \tag{30}$$

1 We have recalculated the exponent of C_{salt} from experimental points in Fig. 6*A* of the paper of Mueller and Rudin. The mean value of the two slopes of Fig. 5 of the same paper was used for the computation of the voltage dependence.

C_{al} and C_{salt} are the concentrations of alamethicin and salt, respectively, in the aqueous phase. We introduce a factor describing the equivalence of voltage and alamethicin concentration with respect to conductance:

$$\alpha^* = \frac{\ln \frac{C''_{al}}{C'_{al}}}{\frac{F}{RT}(V' - V'')}. \tag{31}$$

The indices ′ and ″ refer to two different sets of experimental data. We obtain from Eq. (29): $\alpha^* = \frac{6.5}{9} = 0.72$, and from Eq. (30): $\alpha^* = \frac{5.5}{6} = 0.92$.

If we consider Eq. (23) and assume equilibrium between alamethicin which is adsorbed at the interface and alamethicin in solution, we can express C_{al} by N_S in Eq. (31). Then α of Eq. (28) and α^* of Eq. (31) become nearly equal:

$$\alpha = \alpha^* + \frac{\alpha^* - \alpha_m}{\nu + 1}. \tag{32}$$

(It should be noted that on the basis of the model, the values of α_m are confined to the interval $0 \leq \alpha_m \leq 1$.) Thus, the experimental values of Eisenberg *et al.* (1973) and Mueller and Rudin (1968) are consistent with ours. The $(C_{al})^6$ dependence of the steady-state conductance found by Mueller and Rudin shows the hexameric pore ($\nu = 4$) to be the most probable pore at the voltage-alamethicin concentration range used in their study. In the case of Eisenberg *et al.*, nonameric pores ($\nu = 7$) seem to be formed, although from single pore measurements they could not see more than five conductance states. We think that their procedure to determine the "characteristic voltage" caused an initial overshoot in ν. A similar overshoot has been observed by Baumann and Mueller (*personal communication*) and also by us in certain experiments.

In addition, we introduce a factor describing the equivalence of salt and alamethicin concentration with respect to conductance

$$\delta = \frac{\ln \frac{C''_{al}}{C'_{al}}}{\ln \frac{C'_{salt}}{C''_{salt}}}. \tag{33}$$

We obtain from Eq. (29): $\delta = \frac{4}{9} = 0.44$; and from Eq. (30): $\delta = \frac{4.6}{6} = 0.77$. Our model assumes 1–1 complex formation ($\delta = 1$) of alamethicin and cation. We think that saturation effects account for this discrepancy.

Another question is concerned with the voltage dependence in the presence of bi- or trivalent cations. An exponential dependence of conductance on the valency of the cation has been reported by Cherry, Chapman and Graham (1972), whereas Eisenberg *et al.* (1973) did not observe a difference between Na^+, K^+ or Ca^{++}. We are presently investigating this problem with steady-state fluctuation measurements.

To get a rough estimate for the changes of alamethicin interfacial concentration we compare different Γ values [Eq. (23)] which are calculated according to Eq. (25). One obtains

$$\begin{aligned} &\text{PC} \quad : \Gamma = 70 \\ &\text{PS/30}: \Gamma = 0.48 \\ &\text{PS/50}: \Gamma = 1.9 \\ &\text{PS/pr} \quad \Gamma = 33. \end{aligned}$$

The experimental bulk concentration of alamethicin of Rf 30 was lower by a factor of 5 for phosphatidylserine membranes as compared to experiments with di-(22:1)-lecithin. However, this does not account for the whole decrease of Γ. Alamethicin of Rf 30 may be repelled to some extent by the negative surface charge. This effect seems to be smaller with alamethicin Rf 50 indicating that this molecule may be less negatively charged compared to alamethicin Rf 30.

If we compare the two alamethicin fractions we see no fundamental difference with regard to the pore formation mechanism. There are small changes in Γ, ΔG_R and $k_{\nu,\nu-1}$. If the difference in the rate constants $k_{\nu,\nu-1}$ of the two alamethicin fractions is due to different activation energies we may estimate this difference to be

$$E^{(30)} - E^{(50)} = RT \ln \frac{k_{\nu,\nu-1}^{(50)}}{k_{\nu,\nu-1}^{(30)}} = 0.94 \text{ cal mol}^{-1}. \tag{34}$$

A large increase in Γ by about two orders of magnitude is observed after protamine addition, as can be seen from the above calculated data. As further experiments show (Boheim, *unpublished results*) alamethicin molecules seem to be attached to the positively charged basic protein, which in turn is in adsorption equilibrium with the negatively charged membrane.

The mode of action of protamine is quite complex. Here we mention only that still higher protamine concentrations than those used in this

paper may bring about a large increase of the mean pore state $\bar{\nu}$. We observed up to 10 different conductance states. The cation-to-anion selectivity of these channels depends on their diameter. A small channel should be relatively more permeable to cations than a larger one. Because protamine is adsorbed to some extent to the membrane interface, the surface charge may assume positive values. Thus, as a consequence of the Gouy-Chapman effect we observed a change in the pore state conductances indicating that more anions than cations are transported through large channels, whereas through small channels it is still the reverse. In case of a salt gradient these two pore types show different concentration potentials. We think excitability phenomena of the alamethicin protamine system (Mueller & Rudin, 1968) may be understood on the basis of the proposed variable aggregation model.

Besides the two known mechanisms of ion permeation (mobile carriers and pores of fixed size) a third type is here described. This type involves formation of channels of variable diameter by aggregation of subunits. Because aggregation is easily controlled, this mechanism may be widely used in biological membranes (Gingell, 1973).

I wish to thank Dr. G. Adam and Dr. P. Läuger for helpful discussions. This work has been financially supported by the Deutsche Forschungsgemeinschaft (SFB 138).

References

Bamberg, E., Läuger, P. 1973. Channel formation kinetics of gramicidin A in lipid bilayer membranes. *J. Membrane Biol.* **11**:177

Bamberg, E., Läuger, P. 1974. Temperature-dependent properties of gramicidin A channels. *Biochim. Biophys. (Biomembranes) (In press)*

Bean, R. C., Shepherd, W. C., Chan, H., Eichner, J. T. 1969. Discrete conductance fluctuations in lipid bilayer protein membranes. *J. Gen. Physiol.* **53**:741

Benz, R., Stark, G., Janko, K., Läuger, P. 1973. Valinomycin-mediated ion transport through neutral lipid membranes: Influence of hydrocarbon chain length and temperature. *J. Membrane Biol.* **14**:339

Cherry, R. J., Chapman, D., Graham, D. E. 1972. Studies of the conductance changes induced in biomolecular lipid membranes by alamethicin. *J. Membrane Biol.* **7**:325

Ehrenstein, G., Lecar, H., Nossal, R. 1970. The nature of the negative resistance in bimolecular lipid membranes containing excitability inducing material. *J. Gen. Physiol.* **55**:119

Eisenberg, M. 1972. Voltage gateable ionic pores induced by alamethicin in black lipid membranes. Ph. D. Thesis. California Institute of Technology, Pasadena, Calif.

Eisenberg, M., Hall, J. E., Mead, C. A. 1973. The nature of the voltage-dependent conductance induced by alamethicin in black lipid membranes. *J. Membrane Biol.* **14**:143

Finkelstein, A., Holz, R. 1973. Aqueous pores created in thin lipid membranes by the polyene antibiotics nystatin and amphotericin B. *In:* Membranes, A Series of Advances. G. Eisenman, editor. Vol. II, p. 377. Marcel Dekker, Inc., New York

Gingell, D. 1973. Membrane permeability change by aggregation of mobile glycoprotein units. *J. Theoret. Biol.* **38**:677

Gordon, L. G. M., Haydon, D. A. 1972. The unit conductance channel of alamethicin. *Biochim. Biophys. Acta* **255**:1014

Hladky, S. B., Haydon, D. A. 1970. Discreteness of conductance changes in bimolecular lipid membranes in the presence of certain antibiotics. *Nature* **225**:451

Melling, J., McMullen, A. I. 1974. Abstracts of the IAMS Meeting, Tokyo, September 1974. p. 2421

Mueller, P., Rudin, D. O. 1968. Action potentials induced in bimolecular lipid membranes. *Nature* **217**:713

Payne, J. W., Jakes, R., Hartley, B. S. 1970. The primary structure of alamethicin. *Biochem. J.* **117**:757

Urry, D. W. 1971. The gramicidin A transmembrane channel: A proposed $\pi_{(L,D)}$ helix. *Proc. Nat. Acad. Sci.* **68**:672

Urry, D. W. 1972. Protein conformation in biomembranes: Optical rotation and absorption of membrane suspensions. *Biochim. Bophys. Acta* **265**:115

Urry, D. W., Goodall, M. C., Glickson, J. D., Mayers, D. F. 1971. The gramicidin A transmembrane channel: Characteristics of head-to-head dimerized $\pi_{(L,D)}$ helices. *Proc. Nat. Acad. Sci.* **68**:1907